

Spin superfluidity and coherent spin precession

This article has been downloaded from IOPscience. Please scroll down to see the full text article.

2009 J. Phys.: Condens. Matter 21 164201

(<http://iopscience.iop.org/0953-8984/21/16/164201>)

View [the table of contents for this issue](#), or go to the [journal homepage](#) for more

Download details:

IP Address: 129.252.86.83

The article was downloaded on 29/05/2010 at 19:08

Please note that [terms and conditions apply](#).

Spin superfluidity and coherent spin precession

Yuriy M Bunkov

Institut Neel, CNRS and UJF, BP 166, F-38042, Grenoble, France

E-mail: Yuriy.Bunkov@Grenoble.CNRS.Fr

Received 22 January 2009

Published 31 March 2009

Online at stacks.iop.org/JPhysCM/21/164201

Abstract

The spontaneous phase coherent precession of the magnetization in superfluid $^3\text{He-B}$ was discovered experimentally in 1984 at the Institute for Physical Problems, Moscow by Borovik-Romanov, Bunkov, Dmitriev and Mukharsky and simultaneously explained theoretically by Fomin (Institut Landau, Moscow). Its formation is a direct manifestation of spin superfluidity. The latter is the magnetic counterpart of mass superfluidity and superconductivity. It is also an example of the Bose–Einstein condensation of spin-wave excitations (magnons). The coherent spin precession opened the way for investigations of spin supercurrent magnetization transport and other related phenomena, such as spin-current Josephson effect, process of phase slippage at a critical value of spin supercurrent, spin-current vortices, non-topological solitons (analogous to Q -balls in high energy physics) etc. New measuring techniques based on coherent spin precession made the investigation of mass counterflow and mass vortices possible owing to the spin–mass interaction. New phenomena were observed: mass–spin vortices, the Goldstone mode of the mass vortex with non-axisymmetric core, superfluid density anisotropy etc. Different types of coherent spin precession were later found in superfluid $^3\text{He-A}$ and $^3\text{He-B}$ confined in anisotropic aerogel, in the states with counterflow and in ^3He with reduced magnetization. Finally, spin superfluidity investigations developed the basis for a modern investigation of electron spin supercurrent and spintronics.

(Some figures in this article are in colour only in the electronic version)

1. Introduction

Superfluid ^3He , since its discovery by Osheroff *et al* in 1972 [1], became one of the main systems for experimental studies of quantum fields theories. This is due to the very rich order parameter of the quantum state for triplet Cooper pairing of superfluid ^3He , which exhibits, in addition to superfluid properties, the properties of a magnetically ordered quantum liquid crystal. Owing to the simultaneously broken gauge, spin and orbit symmetries the Cooper pair wavefunction is described, not only by a global phase, but also the phases of rotations about axes in orbital space and spin space. If we can set up a gradient in these phases of the wavefunction, the system responds by flowing in an attempt to iron out the gradients. Spatial gradients of the phase of rotation in orbital space give an additional term to the mass superfluidity, while the spatial gradient of the phase of rotation in spin space provides a new transport process, the spatial transport of magnetization (spin supercurrent). The complexity of the spin supercurrents of these phenomena follows from the fact

that it is the coherent transport of a vector quantity, not a scalar one, as it is for mass and current charges in superfluidity and superconductivity. Consequently the general expression for the spin supercurrent has a tensor form and reads [2]:

$$J_{i\alpha} = \frac{\hbar}{2m} \rho_{ij\alpha\beta} \Omega_{j\beta} \quad (1)$$

where $\rho_{ij\alpha\beta}$ is the spin superfluid density tensor and $\Omega_{j\beta}$ are the phase gradients of the order parameter. In order to observe the spin supercurrent experimentally one should be able to find the experimental conditions which prevent the unwinding of the wavefunction by reorientation of $\rho_{ij\alpha\beta}$.

The spin transport equation (1) plays an essential role in the spin dynamics of ^3He . First of all, the solution of the equations of spin dynamics with the spin transport equations gives the spin-wave spectrum [2]. Here we are interested in solutions which correspond to long distance transport of magnetization by a spin supercurrent. The first attempt to describe this phenomenon was made in [3]. There it was

suggested that the fast magnetic relaxation in $^3\text{He-A}$, observed in [4], can be explained as a transport of magnetization by spin supercurrents away from the sensitive region of the NMR pick-up coils. In fact the fast relaxation in $^3\text{He-A}$ appears due to a process analogous to the Suhl instability in antiferromagnets, as was shown theoretically in [5] and confirmed experimentally in [6]. Furthermore, in [3] the spin supercurrent was treated by direct analogy with superfluid mass current. It should be pointed out, however, that the analogy between the spin supercurrent and the mass supercurrent is limited since magnetization is a vector quantity. Consequently there are no conservation laws for its components, thus spin supercurrents should be treated in relation to very complex spin dynamics, as was done by Fomin [7].

The long distance spin supercurrent transport was found in experiments with superfluid $^3\text{He-B}$. There was observed a redistribution of magnetization, deflected by pulsed NMR, and formation of a domain with coherent precession of magnetization (homogeneously precessing domain (HPD)). It forms in an inhomogeneous magnetic field, and radiates a very long induction decay signal with a frequency changing in time [8]. The HPD forms in a near closed cell in a region of minimum magnetic field [9]. The mechanism of its formation corresponds well to a Bose–Einstein condensation of spin waves (magnons) in a magnetic trap [10].

The spin supercurrent is the result of the stiffness of the spin part of the order parameter. It can be found in any magnetically ordered material. However, it is usually difficult to observe due to different types of instability, as in $^3\text{He-A}$. The spin precession in superfluid ^3He is very stable owing to the very isotropic spin part of the wavefunction. We can visualize the explanation of spin supercurrent by suggesting a four fluid model, in analogy with Landau’s two fluid model. We can describe superfluid ^3He as a mixture of one normal liquid and a three superfluid quantum liquids in different magnetic quantum states.

$$\Psi(\vec{k}) = \Psi_{\uparrow\uparrow}(\vec{k})|\uparrow\uparrow\rangle + \Psi_{\downarrow\downarrow}(\vec{k})|\downarrow\downarrow\rangle + \sqrt{2}\Psi_{\uparrow\downarrow}(\vec{k})|\uparrow\downarrow + \downarrow\uparrow\rangle, \quad (2)$$

where $\Psi_{\uparrow\uparrow}$, $\Psi_{\downarrow\downarrow}$ and $\Psi_{\uparrow\downarrow}$ are the amplitudes associated with the spin substates $|\uparrow\uparrow\rangle$, $|\downarrow\downarrow\rangle$ and $|\uparrow\downarrow + \downarrow\uparrow\rangle$ respectively. The relation between these substates can be described by the vector \vec{d} , which is actually the spin axis of quantization of the Cooper pair state.

$$\Psi(\vec{k}) = \begin{pmatrix} \Psi_{\uparrow\uparrow}(\vec{k}) & \Psi_{\uparrow\downarrow}(\vec{k}) \\ \Psi_{\downarrow\uparrow}(\vec{k}) & \Psi_{\downarrow\downarrow}(\vec{k}) \end{pmatrix} = \begin{pmatrix} -d_x(\vec{k}) + id_y(\vec{k}) & d_z(\vec{k}) \\ d_z(\vec{k}) & d_x(\vec{k}) + id_y(\vec{k}) \end{pmatrix}. \quad (3)$$

The projection of the spin of the Cooper pair on the direction of \vec{d} is equal to zero, similar to the antiferromagnetic vector \vec{l} in antiferromagnets.

The different phases of ^3He have different forms of $\vec{d}(\vec{k})$ presentation. For $^3\text{He-A}$ it is a single vector for all Cooper pairs and its d_z component is equal to zero. This means that the substate $\Psi_{\uparrow\downarrow}$ has zero density and $^3\text{He-A}$ is a mixture of a normal and only two quantum liquids.

The superfluid phase, named $^3\text{He-A}_1$ is induced by a magnetic field near the transition temperature and has only one

magnetic component $\Psi_{\uparrow\uparrow}$. In other words it is a magnetically induced ferromagnetic state. Consequently, there is only one superfluid liquid and the spin transports are bound to a trivial mass superflow.

In $^3\text{He-B}$ the vector \vec{d} is a function of the Cooper pair orbital momentum \vec{k} and is described by the equation: $\vec{d} = \hat{R}(\theta, \vec{n})\vec{k}$ with $\hat{R}(\theta, \vec{n})$ being a rotation matrix about the axis \vec{n} through the angle θ . Therefore, $^3\text{He-B}$ is a unique magnetically ordered substance with a very isotropic state. The spin subsystem and orbit subsystem remain isotropic. What is broken is the relative symmetry between spin and orbit spaces, which is described by the vector \vec{n} .

Let us consider the consequences of a spatially inhomogeneous \vec{d} for the $^3\text{He-A}$ state with a rotation gradient of \vec{d} in the form:

$$d_x + id_y = |d_\perp|e^{i\vec{k}\vec{R}}, \quad (4)$$

where d_\perp is the component of \vec{d} perpendicular to the quantization axis and \vec{k} is the gradient in direction of \vec{R} . We may consider the spin ‘up’ Cooper pairs $\Psi_{\uparrow\uparrow}$ and the spin ‘down’ Cooper pairs $\Psi_{\downarrow\downarrow}$ as two separate superfluids. Therefore, for the function $\Psi_{\downarrow\downarrow}$, we have a phase gradient \vec{k} directed along \vec{R} , while for $\Psi_{\uparrow\uparrow}$ we have the opposite gradient ($-\vec{R}$) and consequently a counterflow of these two superfluids. This counterflow transports magnetization without mass transport and is called the spin supercurrent. This simple model can also be considered for $^3\text{He-B}$, but in this case we should suppose that the counterflow also depends on the momentum in k space. Indeed, after integration over all k , we will have the same spin supercurrent, as follows from Fomin’s theory [7] based on a solution of the antiferromagnetic resonance equations of Leggett [2]. Here we should point out that the four fluid model is only a useful way to visualize the spin supercurrent in superfluid ^3He . Consequently, the spin supercurrent in ^3He is an example of spin supercurrent of a magnetically ordered material, and not only the superfluid one.

The vector \vec{d} is bound to the magnetization. One can produce spatial structures of \vec{d} by NMR. There are two different modes of NMR in superfluid ^3He ; longitudinal NMR and transverse NMR. In the first case the mode of magnetization and orientation of \vec{d} oscillate. At a high enough excitation of this mode, \vec{d} begins to rotate. The longitudinal mode of NMR can also be excited by a first order A–B transition. The equilibrium magnetization changes at the transition. The jump of magnetization locally excites a longitudinal NMR mode. The propagating front of the A–B transition produces a spatial structure of the \vec{d} vector. In particular, at relatively low temperatures, in the conditions of an overcooled A phase, the A–B boundary can move fast, while the magnetic relaxation is small. As a result a spatial structure of \vec{d} , creates spin supercurrents, which redistribute the non-equilibrium magnetization. Magnetic solitons appear, which move even faster than the A–B boundary itself and can be observed far away from the A–B boundary, as was found in the experiments of Boyd and Swift [11]. This phenomenon was explained quantitatively by Bunkov and Timofeevskaya [12] as a result of spin supercurrent flow.

The first evidence of spin supercurrent was found in the experiments with transverse NMR, where the magnetization deflects by a large angle and precess. It must be mentioned that the mode of magnetization of superfluid ^3He is conserved in the adiabatic approximation due to dipole–dipole energy. Consequently the local magnetization can only change the spatial orientation. On the other hand, the component of magnetization along of the magnetic field is a quasi conserved value due to the weakness of the magnetic relaxation. In the presence of a gradient of the external magnetic field a gradient of the phase of precession appears. The orientations of \vec{M} and \vec{d} are closely related. The gradients of the phase of precession α lead to gradients of \vec{d} and consequently to spin supercurrents. As a result of the spin supercurrent the distribution of angles of deflection β also changes. The spin supercurrent of the longitudinal magnetization \vec{J}_P can be described as a function of the gradients of the angle of deflection β and the angle of precession α of the magnetization

$$\vec{J}_P = F_\alpha(\beta)\nabla\alpha + F_\beta(\beta)\nabla\beta. \quad (5)$$

Consequently, to create long-range spin supercurrents in $^3\text{He-B}$ it is necessary to induce spatial gradients in the phase of the precession.

The equations of NMR in ^3He , the so called Leggett equations, are the equations of antiferromagnetic resonance with an anisotropic term due to the nuclear dipole–dipole interaction. The solution of these equations for bulk $^3\text{He-B}$ shows that the magnetization precesses at the Larmor frequency if it is deflected by less than the ‘magic’ dipole angle of 104° . For larger angles of deflection an additional positive frequency shift appears. The spin supercurrent transports the longitudinal component of magnetization in the direction of higher magnetic field. Consequently the deflection of magnetization in the region of smaller magnetic field increases up to a value of 104° . At further deflection, the dipole–dipole frequency shift compensates the gradient of magnetic field. The spatial magnetic energy potential becomes flat and a state with a coherent precession (HPD) forms.

2. Coherent precession as a magnon BEC

The HPD is a dynamical state which experiences the off-diagonal long-range order [13]:

$$\langle \hat{S}_+ \rangle = S_+ = S \sin \beta e^{i\omega t + i\alpha}. \quad (6)$$

Here \hat{S}_+ is the operator of spin creation; $S_+ = S_x + iS_y$; $\vec{S} = (S_x, S_y, S_z = S \cos \beta)$ is the vector of spin density precessing in the applied magnetic field $\vec{H} = H\hat{z}$; β , ω and α are correspondingly the tipping angle, frequency and the phase of precession. In the modes under discussion, the magnitude of the precessing spin S equals an equilibrium value of spin density $S = \chi H/\gamma$ in the applied field, where χ is the spin susceptibility of $^3\text{He-B}$ and γ the gyromagnetic ratio of the ^3He atom. Similar to the conventional mass superfluidity, which also experiences off-diagonal long-range order, the spin

precession in equation (6) can be rewritten in terms of the complex scalar order parameter [14–16]

$$\langle \hat{\Psi} \rangle = \Psi = \sqrt{2S/\hbar} \sin \frac{\beta}{2} e^{i\omega t + i\alpha}. \quad (7)$$

If the spin–orbit interaction is small and its contribution to the spectrum of magnons is neglected in the main approximation (as typically occurs in ^3He), then $\hat{\Psi}$ coincides with the operator of the annihilation of magnons, with the number density of magnons being equal to the condensate density:

$$n_M = \langle \hat{\Psi}^\dagger \hat{\Psi} \rangle = |\Psi|^2 = \frac{S - S_z}{\hbar}. \quad (8)$$

This implies that the precessing states in superfluid ^3He realize an almost complete BEC of magnons. The small spin–orbit coupling produces a weak interaction between magnons and leads to the interaction term in the corresponding Gross–Pitaevskii equation for the BEC of magnons (furthermore we use units with $\hbar = 1$):

$$\frac{\delta F}{\delta \Psi^*} = 0, \quad (9)$$

$$F = \int d^3r \left(\frac{|\nabla\Psi|^2}{2m_M} - \mu|\Psi|^2 + \bar{E}_D(|\Psi|^2) \right). \quad (10)$$

Here the role of the chemical potential $\mu = \omega - \omega_L$ is played by the shift of the precession frequency from the Larmor value $\omega_L = \gamma H$; the latter may slightly depend on coordinates if a field gradient is applied. In coherent states, the precession frequency ω is the same throughout the whole sample, even in non-uniform field; it is determined by the number of magnons in BEC, $N_M = \int d^3r n_M$, which is a conserved quantity if the dipole interaction is neglected. In the regime of continuous NMR, ω is the frequency of the applied RF field, $\omega = \omega_{\text{RF}}$, and the chemical potential $\mu = \omega_{\text{RF}} - \omega_L$ determines the magnon density. Finally, m_M is the magnon mass; and \bar{E}_D the dipole interaction averaged over the fast precession. The general form of $\bar{E}_D(|\Psi|^2)$ depends on the orientation of the orbital degrees of freedom described by the unit vector \hat{l} of the orbital momentum, see [17].

In the coherent precession of bulk $^3\text{He-B}$ the spin–orbit coupling orients the vector \hat{l} along the axis of precession, i.e. $\hat{l} \parallel \vec{H}$. In this case the interaction term \bar{E}_D , expressed through the condensate order parameter, has a form different from the conventional 4th order term in dilute gases [16]:

$$\bar{E}_D = 0, \quad |\Psi|^2 < \frac{5}{4}S, \quad (11)$$

$$\bar{E}_D = \frac{8}{15}\chi\Omega_L^2 \left(\frac{25}{16} - \frac{5|\Psi|^2}{2S} + \frac{|\Psi|^4}{S^2} \right)^2, \quad |\Psi|^2 > \frac{5}{4}S. \quad (12)$$

Here $\Omega_L \ll \omega_L$ is the Leggett frequency which characterizes the dipole interaction. If the chemical potential μ is negative, i.e. ω is less than ω_L , the minimum of the Ginzburg–Landau (GL) energy $\bar{E}_D(|\Psi|^2) - \mu|\Psi|^2$ corresponds to $\Psi = 0$, i.e. to the static state with non-precessing equilibrium magnetization ($\beta = 0$). For $\mu > 0$ (i.e. for positive frequency shift), the profile of the (normalized) energy density is shown in

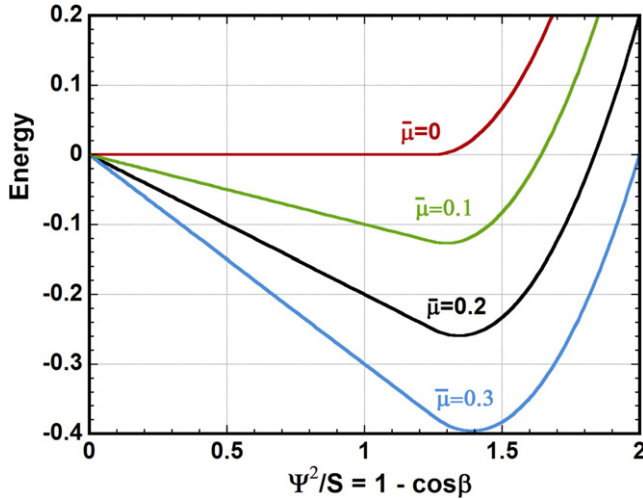


Figure 1. The Ginzburg–Landau energy $\bar{E}_D(|\Psi|^2) - \mu|\Psi|^2$ in bulk $^3\text{He-B}$ as a function of magnon density (tipping angle of precession) for different values of the normalized chemical potential $\bar{\mu} = (\omega_{\text{RF}}^2 - \omega_L^2)/\Omega_L^2$. The energy minima correspond to magnon BEC, i.e. coherent HPD states precessing with a frequency shift equal to the chemical potential.

figure 1 for several values of μ , given in dimensionless units $\bar{\mu} = (\omega_{\text{RF}}^2 - \omega_L^2)/\Omega_L^2 \approx \mu/(\Omega_L^2/2\omega_L)$. The minimum of the GL energy corresponds to $|\Psi|^2/S = (5/4) + (15/32)\bar{\mu}$. The consequence of the peculiar profile of the interaction term is that, distinctly from the dilute gases, the formation of the magnon BEC state (HPD) starts with the finite magnitude $|\Psi|^2 = (5/4)S$. This means that the coherent precession starts with a tipping angle equal to the magic Leggett angle, $\beta = 104^\circ$. Let us now add a gradient of magnetic field. The profile of the energy density for different parts of the cell is shown in figure 2 for the same frequency of NMR precession. The difference between the frequency of precession and the local Larmor frequency leads to a different chemical potential in the top and the bottom of the cell. The position with $\mu = 0$ (position of the HPD domain boundary) is determined by the balance of the longitudinal magnetization in the cell. With relaxation, the longitudinal magnetization increases and, consequently, the boundary moves to lower fields. The HPD state can persist indefinitely, if one applies a small RF field to compensate the losses of magnons caused by the small spin–orbit interaction. In conventional magnetic systems, the magnetization precesses in the local field with the local frequency shift and thus experiences dephasing in an inhomogeneous field. In the case of magnon BEC, the rigidity of the order parameter (the gradient term in equation (10)) plays an important role. The spatial dephasing leads to the gradient of chemical potential. This in turn excites the spin supercurrents, which finally remove the gradient of chemical potential. Finally, the gradient of the local field is compensated by a small gradient of magnon density $|\Psi|^2$ in such a way that the precession frequency and its phase remain homogeneous throughout the whole sample. In a pulsed NMR experiment the magnetization is deflected by a strong RF pulse. The induction decay signal at a given gradient should completely disappear in about 10 ms. Instead, after a transient process

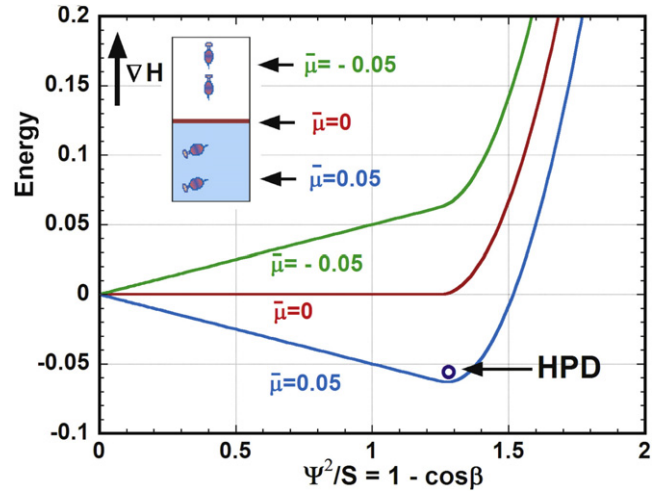


Figure 2. The Ginzburg–Landau energy $\bar{E}_D(|\Psi|^2) - \tilde{\mu}|\Psi|^2$ as a function of magnon density for the cell placed in a gradient of magnetic field ω_L (this corresponds to a gradient of normalized chemical potential $\tilde{\mu} = (\omega^2 - \omega_L^2)/\Omega_L^2$).

of about 2 ms, the induction signal acquires an amplitude corresponding to about 100% of the deflected magnetization with a spontaneously emerging phase, as shown in figure 3. This coherent state lives about 500 times longer than in the non-interacting spin system.

The HPD has been observed, studied and explained on the basis of the theory of spin superfluidity and nonlinear NMR [8]. However, the consideration of this phenomenon in terms of the magnon BEC not only demonstrates a real system with BEC of excitations, but also allows us to simplify the problem and to study and search for other types of magnon BEC in ^3He . New BEC states were discovered: Q -balls [18]; the HPD₂ state in a deformed aerogel [19]; coherent precession in $^3\text{He-A}$ in a deformed aerogel [20]; etc. More detailed explanations of magnon BEC can be found in review articles [10, 16].

3. Demonstration of spin supercurrent

In order to demonstrate the non-potential flow of magnetization, two HPDs were excited in two cylindrical cells by applying two independent RF fields. The cells were placed in the same magnetic field and connected by a channel of 1.4 mm diameter and 7 mm length. The HPD states play the role of electrodes, and the RF field frequency the potential. In the magnetic field the spin current transports the Zeeman energy, which can be measured by the balance of dissipation in the two cells. We have demonstrated spin-current flow, which is determined by the phase gradient of magnetization precession along the channel [21]. We have observed the Josephson phenomenon by adding an orifice inside the channel [22]. The magnetic coherence length of HPD depends on the distance from the HPD boundary and the gradient of magnetic field. We have observed a sinusoidal and deformed phase-current dependence as well as a phase slippage regime by changing the position of the HPD boundary, see figure 4. The detailed explanation of the Josephson experiments and many other experiments, which we have no space to discuss here, can be found in the review article [14].

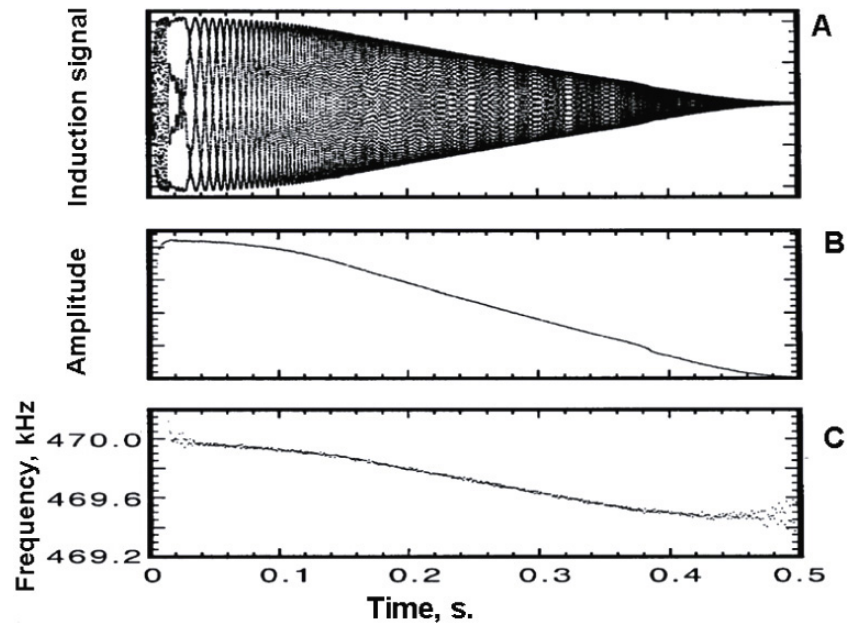


Figure 3. The typical signal of HPD decay; (A) stroboscopic record of the signal; (B) amplitude of signal; (C) frequency of the signal. Frequencies 469.95 and 469.4 kHz correspond to the Larmor frequency at the top and the bottom of the cell.

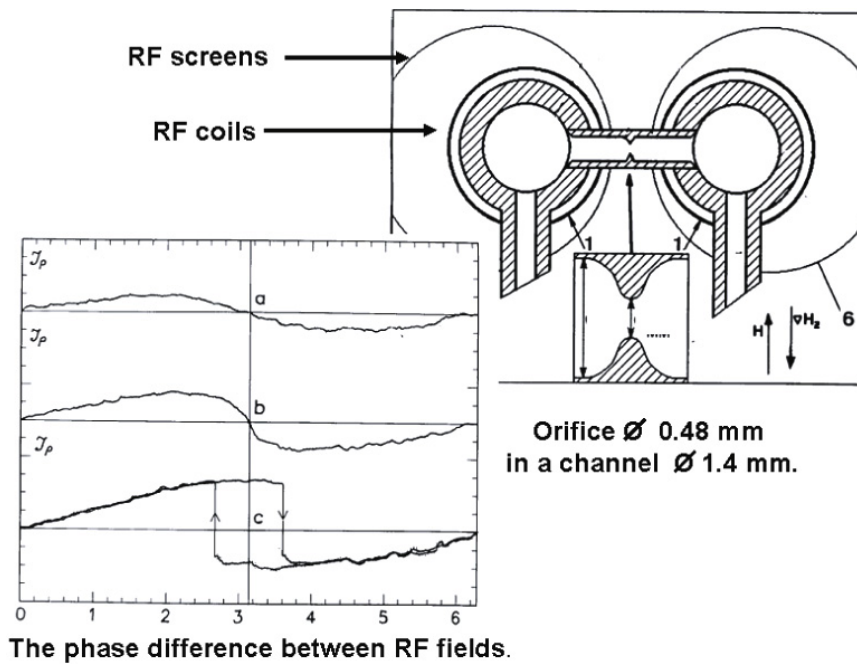


Figure 4. The Josephson experiment. Two NMR cells connected by a channel with a diaphragm. Two independent CW NMR coils control the phase of precession of HPDs. The spin supercurrent through a diaphragm transports the magnetization and, consequently, Zeeman energy. This energy transport was measured by an increase of the adsorption signal in one cell and its decrease in another cell. The records of adsorption signal dependence on the difference between the phase of the HPDs is shown in the inset. (a)—classical Josephson signal, (b)—signal with distortion, (c)—phase slippage.

4. Conclusion

In this short article we were not able to mention all the experiments with spin supercurrent made during the 20 years after its discovery in the Institute for Physical Problems in Moscow by Borovik-Romanov, Bunkov, Dmitriev, Mukharsky and its explanation by Fomin. An outline of the basic theoretical and experimental aspects of the spin supercurrent

can be found in review articles [7, 14] and others. Here we have briefly presented the state of spin superfluidity investigations. First of all, many of the experiments were done in the Institut Neel (ex. CRTBT) in Grenoble, by Bunkov and his collaborators [23]. There is a long history of collaborations between the Institute Kapitza in Moscow and the Low Temperature Laboratory of the Helsinki Technological University, starting with the very successful Soviet-Finnish

project ROTA. In the framework of this project Bunkov and Hakonen [24] have made a pioneering experiments on vortices and counterflow interactions with HPD. Later it was found that HPD supplies a very useful tool for studying the dynamics of superfluid ^3He under rotation. Recently a new magnetic coherent quantum state, ‘ Q ’-ball, has been applied to the study of vortices and counterflow at the limit of very low temperatures. The HPD studies at the limit of ultralow temperatures were done at Lancaster University, UK. NMR in the Landau field [25] and a new state of coherent precession, Persistent signal [26] were observed. Many investigations of HPD dynamics were done by the experimental group from Kosice, Slovakia [27]. The problem of the HPD instability in a wide range of magnetic fields was studied at Cornell University, USA [28]. The HPD in an aerogel under rotation was investigated at Kyoto University and the Institute of Solid State Physics, Kashiva, Japan [20]. Finally, as was mentioned previously, another mode of spin supercurrent was observed at Los-Alamos Laboratory [11].

References

- [1] Osheroff D D, Richardson R C and Lee D M 1972 *Phys. Rev. Lett.* **29** 920
- [2] Leggett A J 1975 *Rev. Mod. Phys.* **47** 331
- [3] Vuorio M 1976 *J. Phys. C: Solid State Phys.* **9** 267
- [4] Corruccini L R and Osheroff D D 1974 *Phys. Rev. Lett.* **34** 564
- [5] Fomin I A 1979 *JETP Lett.* **30** 164
- [6] Bunkov Yu M, Dmitriev V V and Mukharskiy Yu M 1985 *Sov. Phys.—JETP* **61** 719
- [7] Fomin I A 1990 *Helium Three* (Amsterdam: Elsevier) p 609
- [8] Borovik-Romanov A S, Bunkov Yu M, Dmitriev V V and Mukharskiy Yu M 1984 *JETP Lett.* **40** 1033
- [9] Fomin I A 1984 *JETP Lett.* **40** 1037
- [10] Bunkov Yu M and Volovik G E 2008 *J. Low Temp. Phys.* **150** 135
- [11] Boyd S T P and Swift G W 1992 *J. Low Temp. Phys.* **86** 325
- [12] Bunkov Yu M and Timofeevskaya O D 1992 *Phys. Rev. Lett.* **69** 3662
- [13] Bunkov Yu M, Timofeevskaya O D and Volovik G E 1994 *Phys. Rev. Lett.* **73** 1817
- [14] Bunkov Yu M 1995 *Progress in Low Temperature Physics* vol 14 (Amsterdam: Elsevier) p 68
- [15] Fomin I A 1991 *Physica B* **169** 153
- [16] Volovik G E 2007 arXiv:cond-mat/0701180
- [17] Bunkov Yu M and Volovik G E 1993 *JETP* **76** 794
- [18] Bunkov Yu M and Volovik G E 2007 *Phys. Rev. Lett.* **98** 265302
- [19] Elbs J, Collin E, Bunkov Yu M, Godfrin H and Volovik G E 2008 *Phys. Rev. Lett.* **100** 215304
- [20] Sato T, Kunimatsu T, Izumina K, Matsubara A, Kubota M, Mizusaki T and Bunkov Yu M 2008 *Phys. Rev. Lett.* **101** 055301
- [21] Bunkov Yu M 1987 *J. Appl. Phys.* **26** 1809
- [22] Borovik-Romanov A S, Bunkov Yu M, Dmitriev V V, Mukharskiy Yu M and Sergatskov D A 1989 *Phys. Rev. Lett.* **62** 1631
- [23] Bunkov Yu M, Chen A S, Cousins D J and Godfrin H 2000 *Phys. Rev. Lett.* **85** 3456
- [24] Bunkov Yu M and Hakonen P J 1991 *J. Low Temp. Phys.* **83** 323
- [25] Bunkov Yu M, Fisher S N, Guenault A M and Pickett G R 1992 *Phys. Rev. Lett.* **68** 600
- [26] Bunkov Yu M, Fisher S N, Guenault A M and Pickett G R 1992 *Phys. Rev. Lett.* **69** 3092
- [27] Clovecko M, Gazo E, Kupka M and Skiba P 2008 *Phys. Rev. Lett.* **100** 155301
- [28] Geller D A and Lee D M 2000 *Phys. Rev. Lett.* **85** 1032